entropy

MDPI

Article

A Complexity-Based Approach for the Detection of Weak Signals in Ocean Ambient Noise

Shashidhar Siddagangaiah *, Yaan Li *, Xijing Guo, Xiao Chen, Qunfei Zhang, Kunde Yang * and Yixin Yang

School of Marine Science and Technology, Northwestern Polytechnical University, Xi'an 710072, China; xguo@nwpu.edu.cn (X.G.); chenxiao@mail.nwpu.edu.cn (X.C.); zhangqf@nwpu.edu.cn (Q.Z.); yxyang@nwpu.edu.cn (Y.Y.)

* Correspondence: shashi.18j@gmail.com (S.S.); liyaan@nwpu.edu.cn (Y.L.); ykdzym@nwpu.edu.cn (K.Y.); Tel.: +86-29-8849-5817 (S.S. & Y.L.); +86-29-8846-0586 (K.Y.)

Academic Editors: J.A. Tenreiro Machado and António M. Lopes
Received: 17 December 2015; Accepted: 8 March 2016; Published: 18 March 2016

Abstract: There are numerous studies showing that there is a constant increase in the ocean ambient noise level and the ever-growing demand for developing algorithms for detecting weak signals in ambient noise. In this study, we utilize dynamical and statistical complexity to detect the presence of weak ship noise embedded in ambient noise. The ambient noise and ship noise were recorded in the South China Sea. The multiscale entropy (MSE) method and the complexity-entropy causality plane (*C-H* plane) were used to quantify the dynamical and statistical complexity of the measured time series, respectively. We generated signals with varying signal-to-noise ratio (SNR) by varying the amplification of a ship signal. The simulation results indicate that the complexity is sensitive to change in the information in the ambient noise and the change in SNR, a finding that enables the detection of weak ship signals in strong background ambient noise. The simulation results also illustrate that complexity is better than the traditional spectrogram method, particularly effective for detecting low SNR signals in ambient noise. In addition, complexity-based MSE and *C-H* plane methods are simple, robust and do not assume any underlying dynamics in time series. Hence, complexity should be used in practical situations.

Keywords: ambient noise; ship signal; Entropy; complexity; weak signal detection; stochastic dynamics

1. Introduction

The background sound in the ocean is called ambient noise. Ambient noise is constituted by contributions from numerous natural and anthropogenic source. These sounds blend to produce a continuum of noise against which acoustic receivers must be used to detect a signal. Ocean acoustic signals are typically of low signal-to-noise ratio. The received signals are perturbed by varying ambient noise levels with constantly changing factors such as intensity of rainfall, wind speed and its direction, anthropogenic sources, and human-related noises [1–3]. These processes exhibit multiple spatial and temporal variations, strongly affecting ocean acoustic signals. Ambient noise fluctuations are usually nonstationary and nonlinear due to the extraordinary complexity of ocean system [4]. Therefore, it is a challenging task to detect and distinguish the weak acoustic signal in complex ocean ambient noise. It has been reported that, in the past five decades, the artificial low frequency shipping noise radiation has increased by 10–15 dB [5–7]. This has negative implications for mammalian marine wild life [8,9]. Hence, efforts have been made by ship designers and builders to lower the noise produced by their individual ships in some cases to the spectral level of the ambient noise. This may hinder the capability of a traditional spectrum analysis to detect the presence of weak acoustic signals in ambient noise. The

growth in ship and torpedo technology has fueled the demand for more sensitive, reliable, and robust algorithms to detect ever quieter engines in real time and in short time frames [10,11].

A critical assumption in traditional stochastic approach and spectrum analysis is that the spatial and temporal variations of ambient noise are wide-sense stationary. However, nonstationarity and nonlinear effects in these processes need to be considered, which may not be represented by a spectrogram for a stationary process. The ocean acoustic time-series signals measured using underwater sensors remain a largely untapped source of dynamical information. Previous studies on the detection of weak signals in strong ambient noise have assumed that underlying dynamics of ambient noise to be chaotic [12–14]. However, one study [4] showed that ambient noise exhibit neither chaotic nor Gaussian behavior. Instead, ambient noise exhibits nonlinear stochastic behavior. In this study, we utilize complexity, as it does not assume any underlying dynamics; rather, it extracts information from time series. The complexity in ocean acoustic signals can be used as a distinguishing feature to detect the signature of ship and marine mammals. In this study, the dynamical and statistical complexity of ocean acoustic signals is investigated using MSE and *C-H* plane, respectively. Study of entropy-based complexity may offer another way to detect the presence of weak and low SNR signals in background ambient noise. Entropy measures quantify the regularity (predictability) of time series. Traditionally, complexity relates to entropy in the way that entropy increases with the degree of disorder and amounts to a maximum for completely random systems. Dynamical and statistical complexity is quantitative and is based on sample entropy (quantifies the regularity of finite length time series) and Shannon's entropy (quantifies randomness at global level), respectively. The complexity has been successfully applied in the areas, such as medicine [15,16], financial [17,18], climatological [19,20], and acoustic time series [21–23]. From the above examples of the application of complexity, it is clear that it offers a deeper understanding of the properties of time series beyond what can be achieved with other more traditional analysis techniques. The present study, therefore, investigates whether MSE and *C-H* plane-based complexity analysis can be applied to detect the presence of low SNR ship signatures in ambient noise measured at the South China Sea.

The paper is organized as follows. Section 2 describes the measurement of ambient noise and ship signals. Section 3 describes the method for evaluating the dynamical complexity measure (DCM) and the statistical complexity measure (SCM). In Section 4, we explain that we generated signals with different SNRs by varying the amplification of ship signal. Here, we compute spectrogram and complexity measures applied to these signals, and compare the sensitivity of detection of ship signals at a low SNR. Conclusions are stated in Section 5.

2. Data Measurement

The ambient noise and ship signals were recorded in the South China Sea, and the measurements were made using 12 calibrated omnidirectional hydrophones, mounted in a vertical array at a depth of 29 m. The hydrophones used in the experiment have a high sensitivity of -170 dB re 1 V/μPa, provided with an internal 10 dB pre-amplifier with a frequency response between 0.1 Hz$-$80 kHz. The hydrophone was suspended from the ship by a 25-m extension cable. On the deck side, the cable was connected to an input module, which acted as a splitter for signal transfer and the powering of the hydrophone, with a DC supply battery. During recording, there were no observed disturbances from biological or man-made sources. The engines were switched off, and the speed reduced to practically zero. To stretch the hydrophone cable and to assure vertical deployment of the hydrophone, an additional rope was taped along the hydrophone cable, a weight of 1.5 kg underneath the hydrophone. Recordings at two distances, 2.5 km and 1 km away from the hydrophone, were made using the same measurement setup. The experimental vessel was traveling at approximately 20 knots. To avoid interference, it was ensured that, in the radius of about 10 km, no other vessels were present. The data acquired at the sampling rate of 16 kHz over a period of 60 s with 960,000 samples were used for analysis. Figure 1 depicts the recorded ambient noise and ship signals.

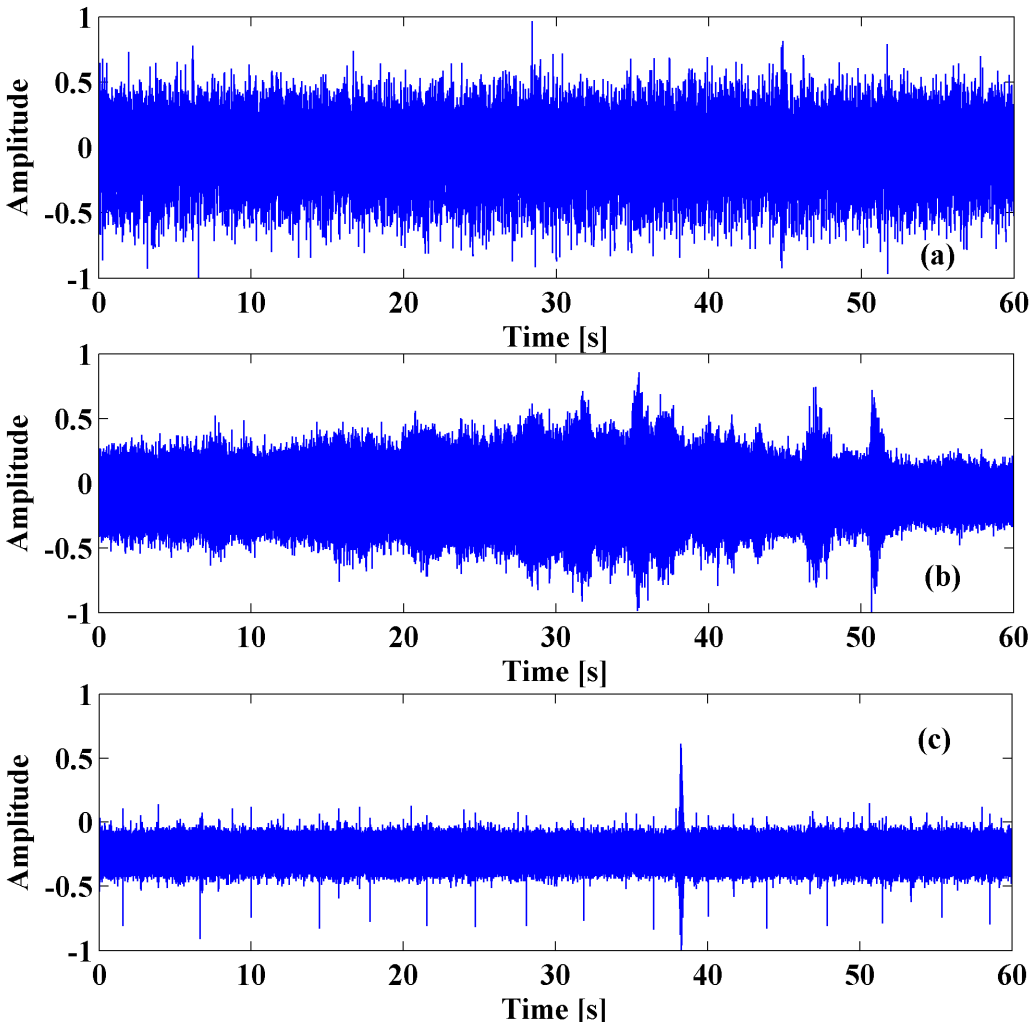

Figure 1. Recordings of (**a**) ocean ambient noise, and (**b**,**c**) the ship at 2.5 km and 1 km away from the hydrophone for a duration of 60 s and a sampling frequency of 16 kHz, respectively.

3. Complexity Methods

3.1. Multiscale Entropy-Based Dynamical Complexity Measure

The MSE method quantifies the dynamical complexity of a time series at multiple temporal scales. MSE is based on the estimation of the sample entropy of an observed time series at different granularities. This is achieved by successively coarse-graining the original time-series data into new coarser scale time series and reanalyzing their sample entropies. By plotting the sample entropy estimates against the temporal scaling parameter (the degree of coarse-graining), the effect of scale on the regularity of patterns in the data can be effectively visualized. Sample entropy quantifies the irregularity of a time series. A detailed description of the MSE method can be found in a previous publication [24].

For the analysis of a one-dimensional discrete time series of N measurements, $[x_1, \ldots, x_i, \ldots, x_N]$, we first construct consecutive coarse-grained time series, $[y\tau^{(\tau)}]$, for different values of the temporal scale factor, τ. First, we divide the original times series into non-overlapping windows of length τ,

trimming any residual $<\tau$ elements at the end of the time series. Second, we average all data points inside each window. The resulting coarse-grained time-series elements are calculated as:

$$y_j^{(\tau)} = \frac{1}{\tau} \sum_{i=(j-1)\tau+1}^{j\tau} x_i \tag{1}$$

for $1 \leqslant j \leqslant N/\tau$.

For scale $\tau = 1$, the coarse-grained time series $[y^{(\tau)}]$ is identical to the original time series. For $\tau > 1$, each coarse-grained time series contains $\left(\frac{N}{\tau}\right)$ elements, *i.e.*, the length of the original time series divided by the scale factor (omitting the remainder of the time series with $<\tau$ elements). It is denoted as $y^\tau = \{y^\tau(1), \ldots, y^\tau(i), \ldots, y^\tau\left(\frac{N}{\tau}\right)\}$. Defining an m-dimensional sequence vector, $\mu^m(i) = \{y^\tau(i), y^\tau(i+1), \ldots, y^\tau(i+m-1)\}$, a distance measure for two vectors $\mu^m(i)$ and $\mu^m(j)$ with the length of m points is defined as $d(i,j) = \max\{|y^\tau(i+k) - y^\tau(j-k)| : 0 \leqslant k \leqslant m-1\}$. The parameter r is defined as the tolerance for accepting matches, and $\mu^m(i)$ is similar with $\mu^m(j)$ when $d(i,j) \leqslant r$. The estimated sample entropy (SE) for each coarse-grained time series $[y^{(\tau)}]$ is plotted as a function of the scale factor τ. Sample entropy depends on two parameters: pattern length m ($m \geqslant 1$) and tolerance level r for similarity comparison. We have evaluated the sample entropy for different combinations of pattern length m ($m = 1, 2, 3, 4$) and for tolerance r varying between $0.1 \leqslant r \leqslant 0.25$. We found that they yield similar results in MSE analysis. In our study, we have used $m = 4$ and $r = 0.15$ [25]. C_{DCM} is calculated as the sum of sample entropy values over a pre-defined range of scales.

3.2. Statistical Complexity Measure (SCM)

The SCM is an information quantifier that enables the quantification of the degree of physical structure and dynamical processes present in a time series [26,27]. Given a probability distribution P of M probabilities associated with time series, the SCM quantifier denoted by C_{SCM} is given by [28]

$$C_{SCM}[P] = Q_j[P, P_e] H_{SCM}[P] \tag{2}$$

where

$$Q_j[P, P_e] = \frac{S[(P + P_e)/2] - S[P]/2 - S[P_e]/2}{Q_{\max}}$$

and $Q_{\max}$ is the maximum possible value of $Q_j[P, P_e]$, obtained when one of the components of P is equal to one, and all the others vanish, *i.e.*,

$$Q_{\max} = -\frac{1}{2}\left[\frac{M!+1}{M!}\log(M!+1) - 2\log(2M!) + \log(M!)\right] \tag{3}$$

The quantity H_{SCM} denotes the amount of disorder given by the normalized Shannon entropy $S/S_{\max}$ [29]. The quantity Q_j is disequilibrium and will be different from zero, if there are more likely states among the accessible ones. The varying range of H_{SCM} $[P]$ is between 0 and 1. When $H_{SCM} \approx 1$, it means that the time series is completely random (for example white noise). When $H_{SCM} \approx 0$, it means that the time series is periodic and deterministic (for example sine signal). When H_{SCM} is between 0 and 1, it mean that there is some kind of underlying dynamics embedded in the time series. In order to evaluate the quantifiers H_{SCM} and C_{SCM}, a probability distribution P should be evaluated from the time series. The Bandt and Pompe [30] methodology was employed in our analysis due to its well-known advantages such as simplicity, robustness, and very fast computational evaluation. To utilize the Bandt and Pompe [30] methodology for evaluating the pdf P, it requires the suitable partitions of M-dimensional embedding space. This is expected to reveal significant details concerning the ordinal structure of a given one-dimensional time series For the time series $\{x_t: t = 1, ..., N\}$, an embedding dimension $M > 1$ and embedding time delay d, we are interested in

"ordinal patterns" of order (length) M generated by $(s) \mapsto (x_{s-(M-1)d}, x_{s-(M-2)d}, \ldots, x_{s-d}, x_s)$. This is assigned to each time s the M-dimensional vector of values at times $s, s-d, \ldots, s-(M-1)d$. Clearly, the greater the M-value, the more of the information in the past is incorporated into our vectors. By "ordinal pattern" related to the time (s), we mean the permutation $\pi = (r_0, r_1, \ldots, r_{M-1})$ defined by $x_{s-r_{M-1}d} \leqslant x_{s-r_{M-2}d} \leqslant, \ldots, \leqslant x_{s-r1} \leqslant x_{s-r0}$. In order to get a unique result, we set $r_i < r_{i-1}$ if $x_{s-ri} = x_{s--ri--1}$. Thus, for all the $M!$ possible permutations π of order M, their associated relative frequencies can be naturally computed by the number of times this particular order sequence is found in the time series divided by the total number of sequences. It is possible to quantify the diversity of the ordering symbols (patterns of length M) derived from a scalar time series by evaluating the permutation entropy [31,32]. The embedding dimension M plays an important role in the evaluation of the appropriate probability distribution because M determines the number of accessible states $M!$ and conditions the minimum acceptable length $N \gg M!$ of the time series that one needs in order to work with reliable statistics [25]. In our study, we have considered $M = 4$ and $d = 1$. Bandt and Pompe suggested working with $4 \leqslant M \leqslant 6$ and specifically considered an embedding delay $d = 1$ [30]. It has been recently shown that this parameter is strongly related, if it is relevant, to the intrinsic time scales of the system under analysis [33,34].

The SCM is not a trivial function of the entropy because it depends on two different probability distributions: the one associated to the system under analysis, P, and the uniform distribution, P_e. Furthermore, it was shown that, for a given H_{SCM} value, there is a range of possible C_{SCM} values [35]. Thus, it is clear that C_{SCM} carries important information on correlation structures between the components of the physical system. A detailed analysis of the statistical complexity behavior demonstrates the existence of bounds to C_{SCM} that we called $C_{\max}$ and $C_{\min}$. These bounds can be systematically evaluated, by recourse to a careful geometrical analysis performed in the space of probabilities (P, Ω), where Ω is the sample space [29]. The corresponding values of $C_{\max}$ and $C_{\min}$ depend only on the probability space's dimension and on the functional form adopted by the amount of disorder H_{SCM} and the disequilibrium Q_j. The C-H causality plane is the representation space, obtained by plotting the permutation statistical complexity C_{SCM} *vs.* permutation entropy H_{SCM} of the system. The term causality denotes that the temporal correlation between successive samples is taken into account by using the permutation probability distribution to estimate both quantifiers.

4. Simulation Results

For the purpose of complexity analysis of ocean acoustic data, we simulated signals with varying SNR. To generate signals with varying SNR, we used recorded ship noise as a signal and background ambient noise to represent noise. In this paper, we are verifying the sensitivity of complexity methods for the detection of a low SNR signal. Hence, we consider the ship signal recorded 2.5 km away from the hydrophone. Table 1 shows the resulting SNR for various combinations of ship signals with ambient noise. By varying the amplification of the ship signal, different signals of varying SNRs are generated. We followed this approach because it is challenging to record ships located at great distances since the estimation of accurate SNRs becomes difficult due to a constantly varying ocean environment. We considered that the recording of ships at distant locations may result in interference from other sources. In order to avoid this, we opted to carry out the recording in a well-known and isolated location. Firstly, we computed the spectrogram of the simulated signal. A spectrogram is a visual representation of the distribution of acoustic energy across frequencies and over time. The horizontal axis represents the discrete frequency steps, the vertical axis of a spectrogram typically represents time, and the amount of power is represented as the intensity at each time-frequency point [36]. The principle source of complexity in the analysis of passive sonar-recorded acoustic signal is that all noise from each source in the underwater environment is received. This results in the presence of a large amount of nonlinear and nonstationary ambient background broadband noise in the spectrogram. This noise distorts a ship's signature, causing them to break, particularly at low frequency ranges, and may introduce points of high energy at spurious frequencies. Identifying these

from true signals is particularly hard at low-SNR conditions. As is evident from the spectrogram in Figure 2, as the SNR decreases, the ship tracks, particularly at low frequencies, are not unrecognizable in background ambient noise. It is evident from the spectrogram that, when SNR = −14.4 dB, almost the entire prominent signature of ship tracks is masked by ambient noise.

Table 1. Resulting SNR for various percentages of ship signals in ocean ambient noise.

Percentage of Ship Signal in Ambient Noise	SNR (dB)
100	0.9
90	−0.4
25	−5.1
10	−9.1
3	−14.4
1	−19.2

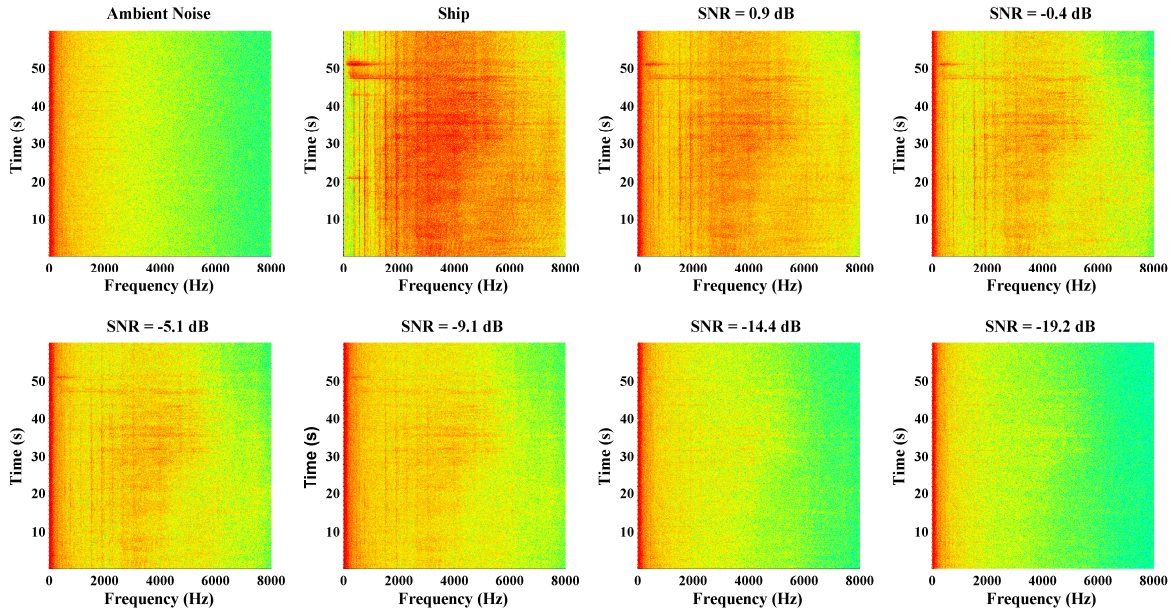

Figure 2. Spectrogram of ambient noise, the ship signal, and varying SNRs of the ship signal.

Next, we evaluated the normalized Shannon's entropy H_{SCM} and statistical complexity C_{SCM} for different varying SNR signals. Figure 3a displays the location of ship, ambient noise, and the varying SNRs of the ship signal on the *C*-*H* plane $H_{SCM} \times C_{SCM}$. It can be noticed that there is a distinct value of H_{SCM} and C_{SCM} for every changing SNR of the ship signal. As the SNR of the ship signal diminishes, the dynamics of the weak ship signal approaches the dynamics of ambient noise. As shown in Figure 3a, on the *C*-*H* plane, it can be observed that the ambient noise has higher H_{SCM} (more stochastic) [37] compared to that of the ship signal. It can be clearly observed in Figure 3b,c that there is a loss of statistical complexity as the SNR decreases. This loss of statistical complexity as SNR decreases enables the detection of the weak ship signal in ambient noise. In Figure 3a,b, it is evident that there is a complexity difference between the ship signal at SNR −19.2 dB (1% of the ship signal in ambient noise) and ambient noise. This feature of complexity difference enables the detection of weak ship noise. However, it can be observed from spectrogram in Figure 2 that, beyond −14.4 dB, the presence of the ship signal is not recognizable in ambient noise. One study [38] has shown that SNR has good agreement with SCM. This feature enabled the SCM to describe stochastic resonance by comparing with the SNR [38]. To ensure that the results presented in Figure 3 are not due to stochastic fluctuations, we computed H_{SCM} and C_{SCM} for the ship signal at −19.2 dB and ambient noise at every 9 s (60 s duration, segregated to form seven signals, each of duration 9 s). In Figure 4,

the computed values of H_{SCM} and C_{SCM} are plotted on the *C*-*H* plane, and it can be observed that a line of threshold can clearly be drawn on the *C*-*H* plane to distinguish the presence of a weak ship signal (−19.2 dB) from ambient noise. Next, we verify how the complexity on the *C*-*H* plane varies for the ambient noises recorded at the depths of 29 m, 50 m, 75 m, 160 m, and 430 m. In Figure 5, it can be clearly seen that the dynamics of ambient noises lie in the stochastic region of the *C*-*H* plane [37], and on average they have similar dynamics. This conclusion agrees with another study [4], which showed the existence of nonlinear stochastic fluctuation in ambient noise.

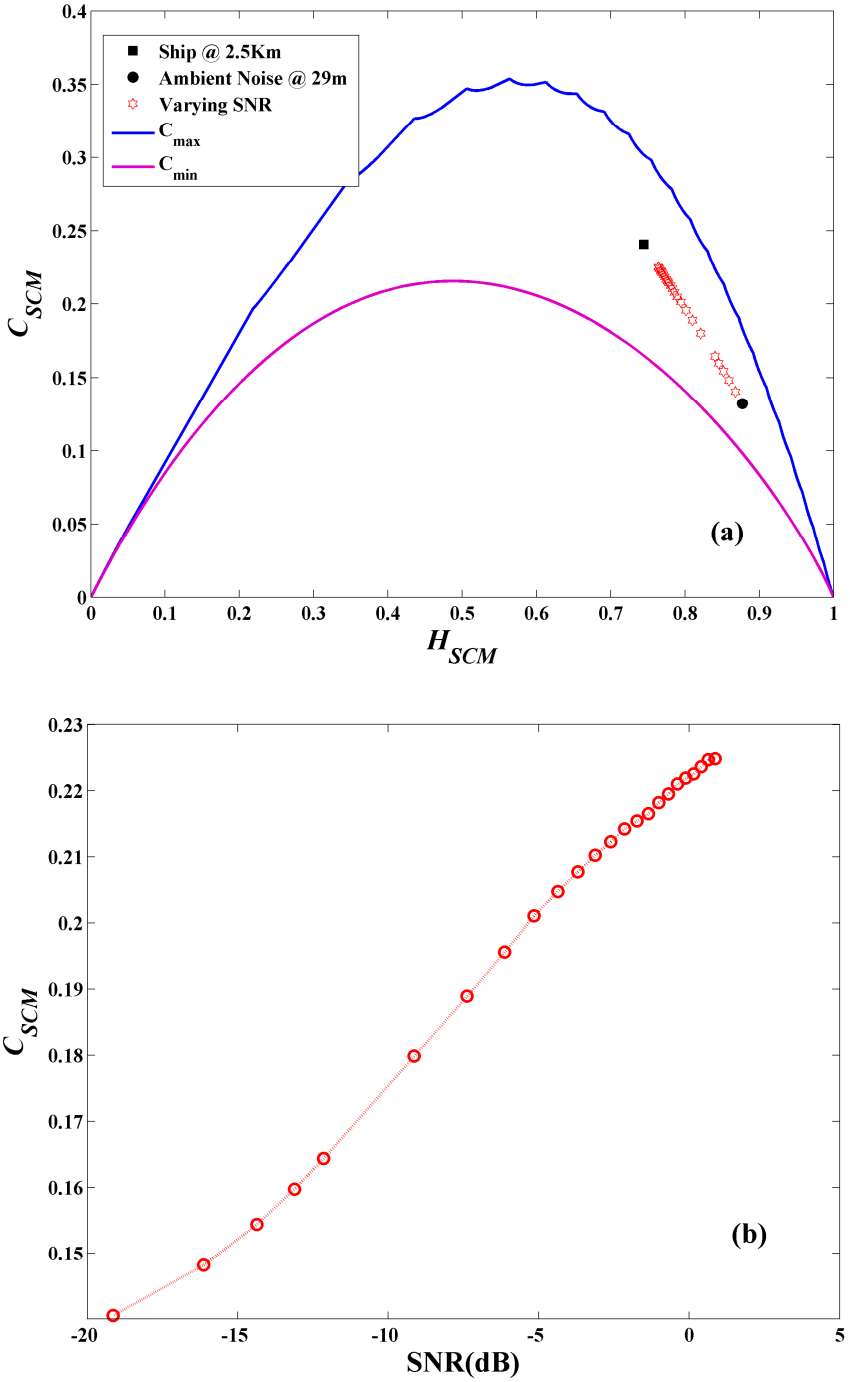

Figure 3. *Cont.*

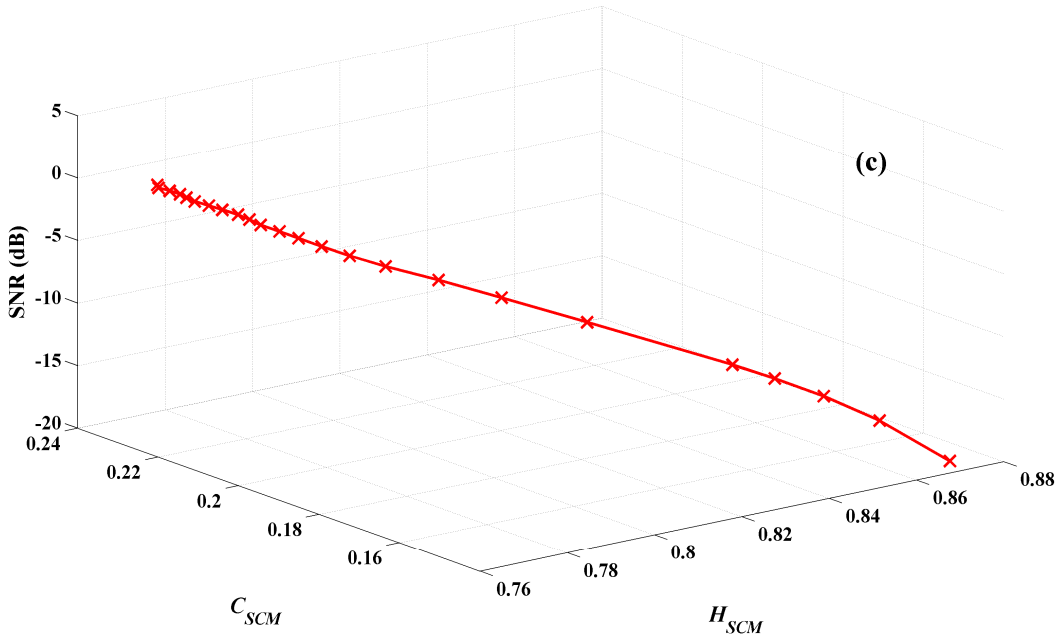

Figure 3. (**a**) Location of ambient noise, ship and varying SNRs of the ship on the *C*-*H* plane, the upper (lower) line represent the maximum (minimum) values of C_{SCM} as a function of H_{SCM} for $M = 4$; (**b**) Representation of variation of statistical complexity measure as a function of varying SNRs of the ship; (**c**) Representation of variation of statistical complexity measure and entropy as a function of varying SNRs of the ship.

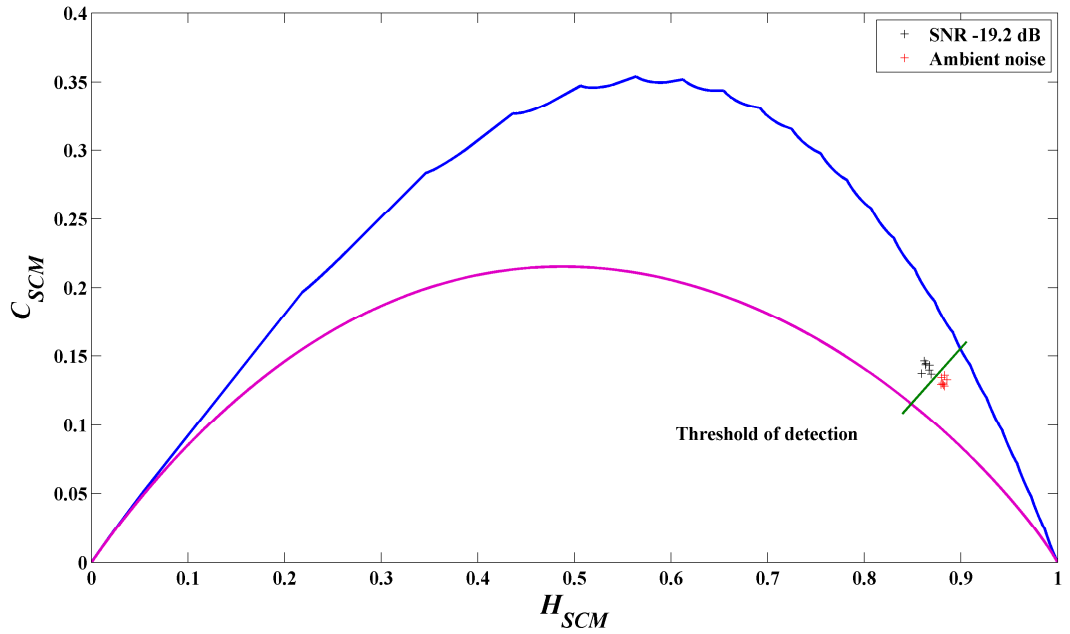

Figure 4. Represents the location of ambient noise and ship signal with SNR −19.2 dB on the *C*-*H* plane, the upper (lower) line represent the maximum (minimum) values of C_{SCM} as a function of H_{SCM} for $M = 4$. The red line represent the threshold of detection between ship signal and ambient noise.

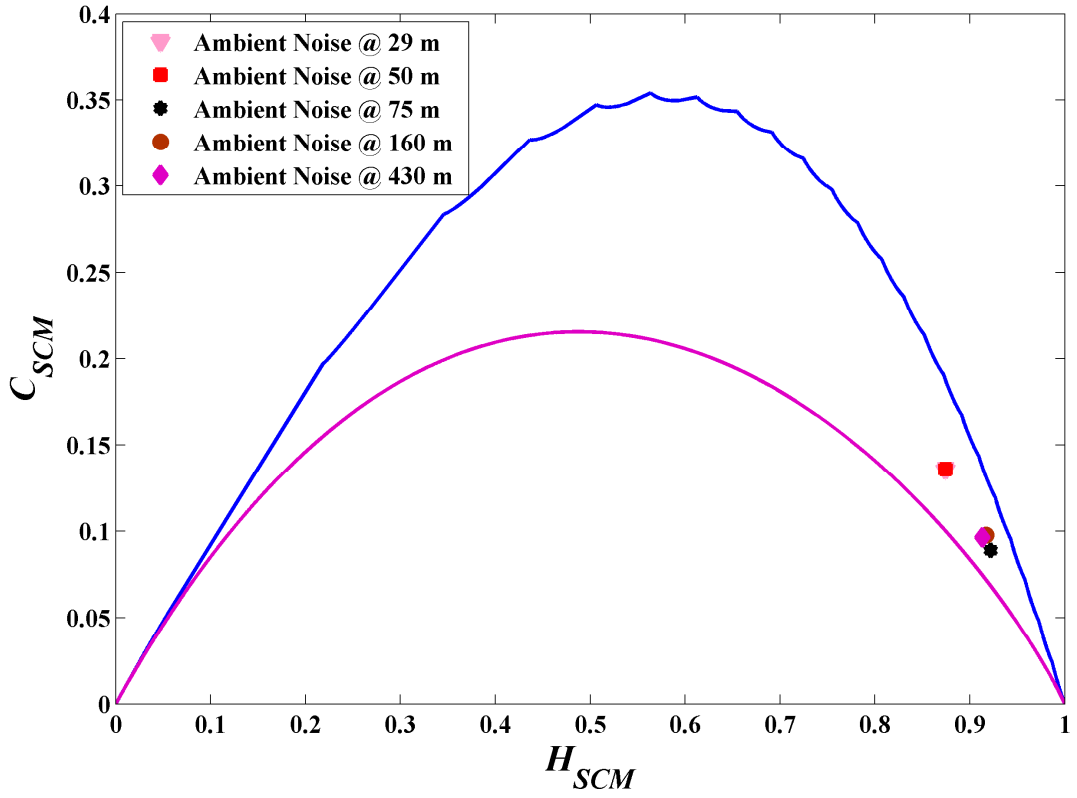

Figure 5. Location of various ambient noises on the *C-H* plane. The upper (lower) line represents the maximum (minimum) values of C_{SCM} as a function of H_{SCM} for $M = 4$.

After verifying the complexity behavior of different ambient noises on the *C-H* plane, we then considered the ship signal recorded at 1 km away and ambient noise recorded at the depth of 75 m to verify the variation of statistical complexity with respect to varying SNRs of the ship signal. Figure 6a displays the location of the ship, ambient noise, and varying SNRs of the ship signal on the *C-H* plane $H_{SCM} \times C_{SCM}$. In Figure 6a, on the *C-H* plane, it can be seen that the ship signal considered in this case is more random and less complex compared to that of the ship signal considered in Figure 3a. Due to the lower C_{SCM} of the ship signal compared to ambient noise, the location of the ship signal on the *C-H* plane is below the ambient noise, which is reciprocal of the case considered in Figure 3a. As a result, it can be seen in Figure 6b that the C_{SCM} is increasing as SNR increases. From the above two cases, it is clear that the location of complexity on the *C-H* plane may vary for different recordings of ambient noise and ship signal; it depends on the dynamics of the ambient noise and ship signal. Complexity may increase or decrease with varying SNRs. However, there will be a complexity change with varying SNRs, which will enable the detection of weak ship signal embedded in ambient noise.

Further, we applied the MSE method for evaluating the DCM of simulated signals. The sample entropy is evaluated for $m = 4$ and $\tau = 1$ for scale factor 1–20. In Figure 7a, we can observe three different types of behavior: (1) The entropy measure of the actual ship signal increases on small time scales [1–5] and decreases on a large time scale [6–20]; (2) the entropy measure for ambient noise monotonically increases with time scale; (3) when the SNR of the ship signal is above −5.1 dB, the entropy curves resemble the ship's dynamics (*i.e.*, entropy increases at small time scales and decreases at higher time scales). However, as the SNR of the ship signal decreases beyond −5.1 dB, the entropy curve resembles that of ambient noise dynamics (monotonic increase of entropy over the entire range of the time scale). This similar shifting in dynamics as the SNR of the ship reduces can be observed in Figure 3a. The MSE method indicates that ship dynamics are more complex; as the SNR of the ship signal reduces, there is a loss of complexity. This loss of dynamical complexity as the SNR of the ship

signal reduces can be clearly seen in Figure 7b. This behavior is similar to that shown in Figure 3b,c. These results exhibit that MSE is capable of detecting the ship signal, even when the ship signal is distorted with 99% of ambient noise (SNR = −19.2 dB). As shown in Figure 7b, the high SNR signals have high dynamical complexity index, which reduces as the SNR decreases. A similar behavior can be observed in Figure 3b where SCM decreases as SNR reduces.

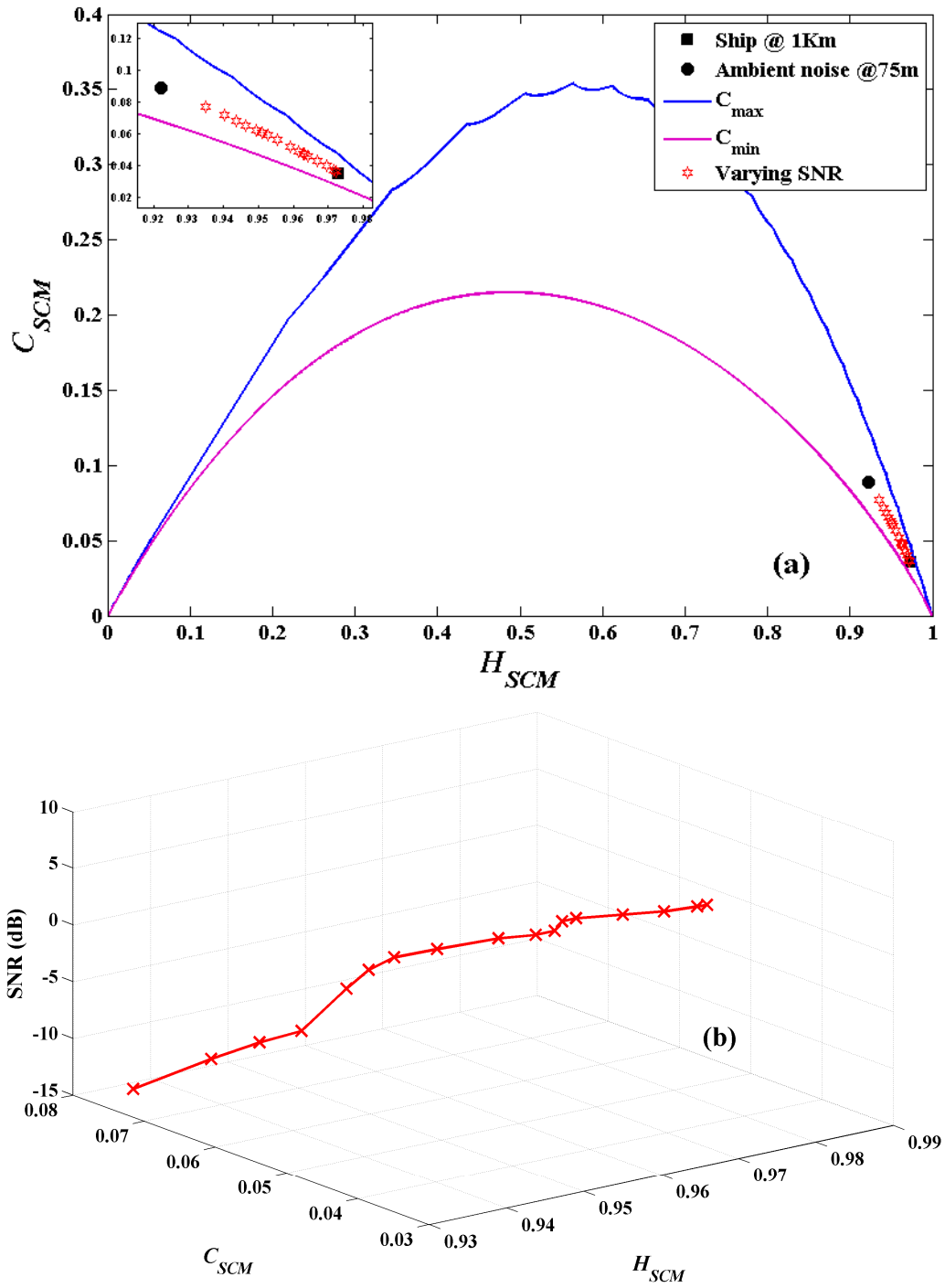

Figure 6. (**a**) Location of ambient noise, ship and varying SNRs of the ship on the *C*-*H* plane. the upper (lower) line represents the maximum (minimum) values of C_{SCM} as a function of H_{SCM} for $M = 4$; (**b**) representation of variation of statistical complexity measure and entropy as a function of varying SNRs of the ship.

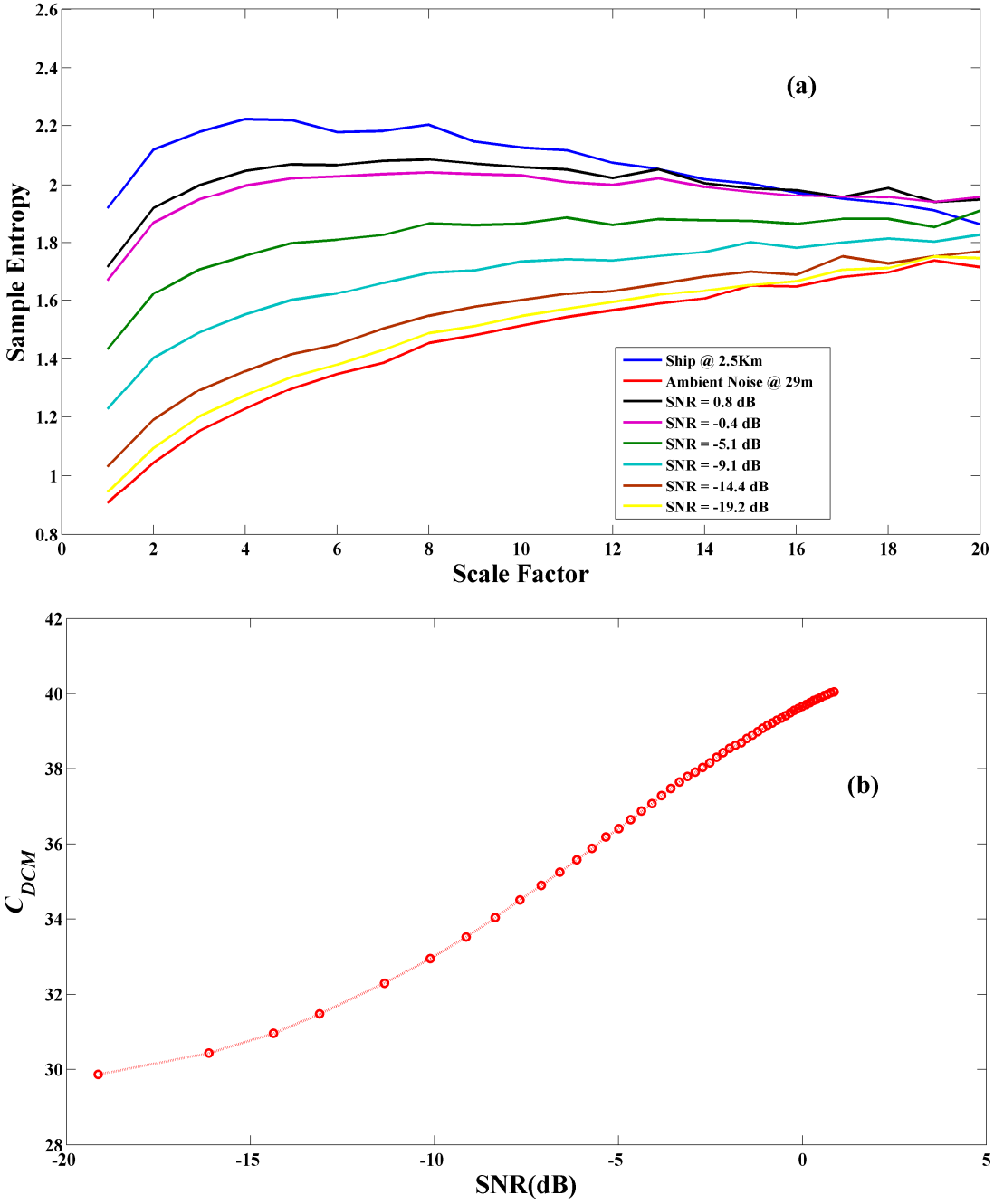

Figure 7. (**a**) MSE analysis of ship signal with varying SNRs evaluated for m = 4 and r = 0.15; (**b**) dynamical complexity measure (sum of sample entropy values for scale 1–20, inclusively) *vs.* varying SNRs of the ship signal.

Figure 8 represents the normalized complexity of SCM and DCM as a function of the SNR and the percentage of ship signal in ambient noise. It can be observed that they have similar sensitivity to the change in SNR. It can be seen that when SNR is below −5 dB, both SCM and DCM have the same complexity. As SNR decreases beyond −5 dB, DCM and SCM deviate, but yet have similar sensitivities to the change in SNR. It can be observed that, when the SNR is higher than −5 dB, the change of complexity is slower, whereas the complexity change is faster for SNRs lower than −5 dB. This varying rate of complexity is due to the change in underlying dynamics of the signal based on the amount of ship signal present. Thus, the complexity measure is sensitive to changes in SNR and can

efficiently detect the presence of any weak extrinsic artifacts, such as ship noise and marine mammals, in ocean ambient noise.

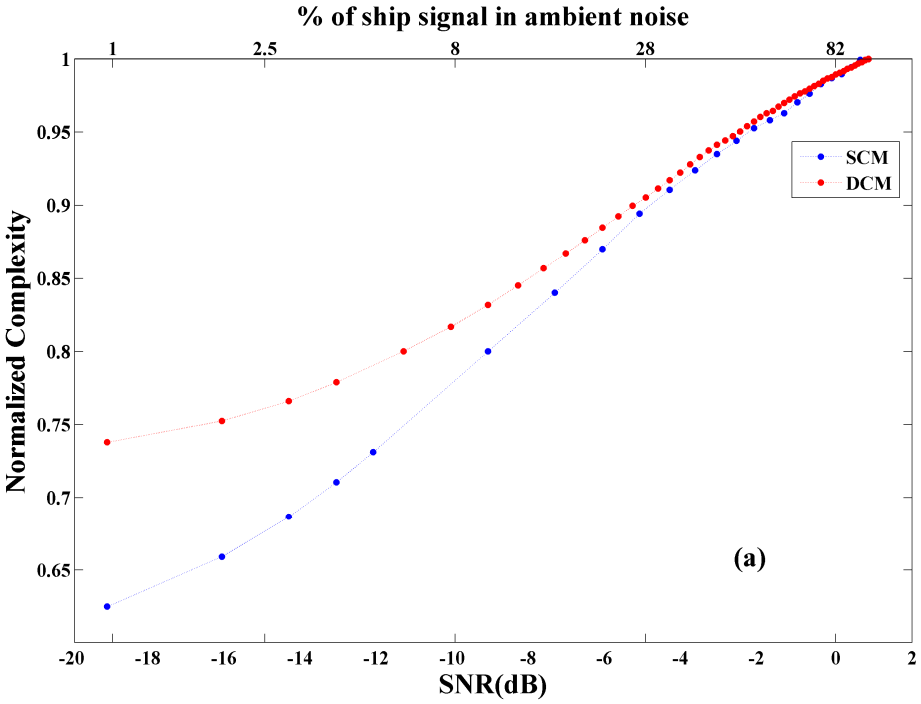

Figure 8. Representation of normalized DCM and SCM as a function of varying SNRs of the ship signal and percentage of ship signal in ambient noise respectively.

5. Conclusions

The ocean acoustic time-series signals measured using underwater sensors remain a largely untapped source of dynamical information. In this work, we evaluated statistical and dynamical complexity by employing the *C-H* plane and MSE, respectively. The results obtained demonstrate that complexity is sensitive to the change in information in the ambient noise. It is shown that there is a loss of complexity and change in underlying dynamics as the SNR of a ship signal is reduced. This feature enables the detection of ship signals distorted by 99% (−19.2 dB) of ambient noise. Complexity analysis can thus detect properties of ocean acoustic time series that are undetectable by the traditional spectrogram method. We report, having used DCM and SCM analysis for the first time to our knowledge, that the complexity of the ocean acoustic time series can be used to detect the presence of weak ship signatures in background ambient noise. These findings indicate that complexity measures can be used as a complementary approach, alongside those taken via traditional spectrogram, for the detection of weak signals in ambient noise. Further work should be taken up to determine the relationship between the variation of complexity and the varying range of the target.

Acknowledgments: This work was supported in part by Grant Nos. 51179157, 11574250 and 11304251 from NSFC China. Shashidhar Siddagangaiah also would like to acknowledge the Chinese Scholarship Council (CSC) for financial support. The authors are pleased to acknowledge useful conversations with Narasimhiah Ramesh. We also gratefully acknowledge the comments of two anonymous reviewers, whose remarks significantly improved the article. The authors would like to acknowledge Key Laboratory of Ocean Acoustics and Sensing (Northwestern Polytechnical University), Ministry of Industry and Information Technology, Xi'an for providing financial support.

Author Contributions: Shashidhar Siddagangaiah, Xijing Guo and Yaan Li conceived and designed the project; Shashidhar Siddagangaiah and Xijing Guo performed the computational analysis; Shashidhar Siddagangaiah wrote the manuscript with the input from Xijing Guo; Yaan Li, Yixin Yang, and Kunde Yang evaluated the manuscript; Xiao Chen, Qunfei Zhang, Kunde Yang, and Yixin Yang, performed the experiments and collected the data. All co-authors reviewed and approved the final manuscript.

Conflicts of Interest: The authors declare no conflict of interest.

References

1. Cato, D.H. A Perspective on 30 Years of Progress in Ambient Noise: Source Mechanisms and the Characteristics of the Sound Field. In Proceedings of the 3rd International Conference on Ocean Acoustics (OA2012), Beijing, China, 21–25 May 2012.
2. Urick, R.J. *Principles of Underwater Sound*, 3rd ed.; McGraw-Hill: New York, NY, USA, 1983.
3. Wagstaff, R.A. An ambient noise model for the northeast Pacific Ocean basin. *IEEE J. Ocean. Eng.* **2005**, *30*, 286–294. [CrossRef]
4. Siddagangaiah, S.; Li, Y.; Guo, X.; Yang, K. On the Dynamics of Ocean Ambient Noise: Two Decades Later. *Chaos* **2015**, *25*. [CrossRef] [PubMed]
5. Clark, C.W.; Ellison, W.T.; Southall, B.L.; Hatch, L.; van Parijs, S.; Frankel, A.; Ponirakis, D. Acoustic masking in marine ecosystems: Intuitions, analysis, and implication. *Mar. Ecol. Prog. Ser.* **2009**, *395*, 201–222. [CrossRef]
6. Donald, R. *Mechanics of Underwater Noise*; Elsevier: Amsterdam, The Netherlands, 2013.
7. Hildebrand, J.A. Anthropogenic and natural sources of ambient noise in the ocean. *Mar. Ecol. Prog. Ser.* **2009**, *395*, 5–20. [CrossRef]
8. Mellinger, D.K.; Nieukirk, S.L.; Matsumoto, H.; Heimlich, S.L.; Dziak, R.P.; Haxel, J.; Fowler, M.; Meinig, C.; Miller, H.V. Seasonal occurrence of North Atlantic Right Whale (*Eubalaena glacialis*) vocalizations at two sites on the Scotian Shelf. *Mar. Mamm. Sci.* **2007**, *23*, 856–867. [CrossRef]
9. Urazghildiiev, I.R.; Clark, C.W. Acoustic detection of North Atlantic Right Whale contact calls using spectrogram-based statistics. *J. Acoust. Soc. Am.* **2007**, *122*, 769–776. [CrossRef] [PubMed]
10. Kozaczka, E.; Grelowska, G. Shipping noise. *Arch. Acoust.* **2004**, *29*, 169–176.
11. Lampert, T.A.; O'Keefe, S.E.M. On the detection of tracks in spectrogram images. *Pattern Recognit.* **2013**, *46*, 1396–1408. [CrossRef]
12. Pan, J.; Jin, H.; Yang, S.-E. A neural network based method for detection of weak underwater signals. *J. Mar. Sci. Appl.* **2010**, *9*, 256–261. [CrossRef]
13. Zheng, S.Y.; Guo, H.; Li, Y.; Wang, B.; Zhang, P. A new method for detecting line spectrum of ship-radiated noise using Duffing oscillator. *Chin. Sci. Bull.* **2007**, *52*, 1906–1912. [CrossRef]
14. Zhang, R.; Chu, F.; Ran, L.; Guo, J. Weak Signal Detection Method under the Strong Noise Background. In Proceedings of the 2011 International Conference on Informatics, Cybernetics, and Computer Engineering (ICCE2011), Melbourne, Australia, 19–20 November 2011; Springer-Verlag: Berlin/Heidelberg, Germany, 2012.
15. Nicolaou, N.; Georgiou, J. The use of permutation entropy to characterize sleep electroencephalograms. *Clin. EEG Neurosci.* **2011**, *42*, 24–28. [CrossRef] [PubMed]
16. Costa, M.D.; Henriques, T.; Munshi, M.N.; Segal, A.R.; Goldberger, A.L. Dynamical glucometry: Use of multiscale entropy analysis in diabetes. *Chaos* **2014**, *24*. [CrossRef] [PubMed]
17. Zunino, L.; Tabak, B.M.; Serinaldi, F.; Zanin, M.; Pérez, D.G.; Rosso, O.A. Commodity predictability analysis with a permutation information theory approach. *Phys. A Stat. Mech. Appl.* **2011**, *390*, 876–890. [CrossRef]
18. Xia, J.; Shang, P.; Wang, J.; Shi, W. Classifying of financial time series based on multiscale entropy and multiscale time irreversibility. *Phys. A Stat. Mech. Appl.* **2014**, *400*, 151–158. [CrossRef]
19. Barreiro, M.; Marti, A.C.; Masoller, C. Inferring long memory processes in the climate network via ordinal pattern analysis. *Chaos* **2011**, *21*. [CrossRef] [PubMed]
20. Balzter, H.; Tate, N.J.; Kaduk, J.; Harper, D.; Page, S.; Morrison, R.; Muskulus, M.; Jones, P. Multi-Scale Entropy Analysis as a Method for Time-Series Analysis of Climate Data. *Climate* **2015**, *3*, 227–240. [CrossRef]
21. Ribeiro, H.V.; Zunino, L.; Mendes, R.S.; Lenzi, E.K. Complexity-entropy causality plane: A useful approach for distinguishing songs. *Phys. A Stat. Mech. Appl.* **2012**, *391*, 2421–2428. [CrossRef]
22. Mendes, R.S.; Ribeiro, H.V.; Freire, F.C.M.; Tateishi, A.A.; Lenzi, E.K. Universal patterns in sound amplitudes of songs and music genres. *Phys. Rev. E* **2011**, *83*. [CrossRef] [PubMed]
23. Ribeiro, H.V.; de Souza, R.T.; Lenzi, E.K.; Mendes, R.S.; Evangelista, L.R. The soundscape dynamics of human agglomeration. *New J. Phys.* **2011**, *13*. [CrossRef]

24. Costa, M.; Goldberger, A.; Peng, C.-K. Multiscale entropy analysis of biological signals. *Phys. Rev. E* **2005**, *71*. [CrossRef] [PubMed]
25. Richman, J.S.; Moorman, J.R. Physiological time-series analysis using approximate entropy and sample entropy. *Am. J. Physiol.* **2000**, *278*, H2039–H2049.
26. Lamberti, P.W.; Martin, M.T.; Plastino, A.; Rosso, O.A. Intensive entropic non-triviality measure. *Phys. A Stat. Mech. Appl.* **2004**, *334*, 119–131. [CrossRef]
27. Martin, M.T.; Plastino, A.; Rosso, O.A. Statistical complexity and disequilibrium. *Phys. Lett. A* **2003**, *311*, 126–132. [CrossRef]
28. Lopez-Ruiz, R.; Mancini, H.L.; Calbet, X. A statistical measure of complexity. *Phys. Lett. A* **1995**, *209*, 321–326. [CrossRef]
29. Shannon, C.E. A mathematical theory of communication. *ACM SIGMOB. Mob.Comput. Commun. Rev.* **2001**, *5*, 3–55. [CrossRef]
30. Christoph, B.; Pompe, B. Permutation entropy: A natural complexity measure for time series. *Phys. Rev. Lett.* **2002**, *88*. [CrossRef]
31. Amigó, J. *Permutation Complexity in Dynamical Systems: Ordinal Patterns, Permutation Entropy and All That*; Springer Science & Business Media: New York, NY, USA, 2010.
32. Zanin, M.; Zunino, L.; Rosso, O.A.; Papo, D. Permutation entropy and its main biomedical and econophysics applications: A review. *Entropy* **2012**, *14*, 1553–1577. [CrossRef]
33. Zunino, L.; Soriano, M.C.; Fischer, I.; Rosso, O.A.; Mirasso, C.R. Permutation-information-theory approach to unveil delay dynamics from time-series analysis. *Phys. Rev. E* **2010**, *82*. [CrossRef] [PubMed]
34. Soriano, M.C.; Zunino, L.; Rosso, O.A.; Fischer, I. Time scales of a chaotic semiconductor laser with optical feedback under the lens of a permutation information analysis. *IEEE J. Quantum Electron.* **2011**, *47*, 252–261. [CrossRef]
35. Martin, M.T.; Plastino, A.; Rosso, O.A. Generalized statistical complexity measures: Geometrical and analytical properties. *Phys. A Stat. Mech. Appl.* **2006**, *369*, 439–462. [CrossRef]
36. Lampert, T.A.; O'Keefe Simon, E.M. A survey of spectrogram track detection algorithms. *Appl. Acoust.* **2010**, *71*, 87–100. [CrossRef]
37. Rosso, O.A.; Larrondo, H.A.; Martin, M.T.; Plastino, A.; Fuentes, M.A. Distinguishing noise from chaos. *Phys. Rev. Lett.* **2007**, *99*. [CrossRef] [PubMed]
38. He, M.; Xu, W.; Sun, Z. Dynamical complexity and stochastic resonance in a bistable system with time delay. *Nonlinear Dyn.* **2015**, *79*, 1787–1795. [CrossRef]

© 2016 by the authors; licensee MDPI, Basel, Switzerland. This article is an open access article distributed under the terms and conditions of the Creative Commons by Attribution (CC-BY) license (http://creativecommons.org/licenses/by/4.0/).